ARTICLE
Journal of Cellular Biochemistry 108:1012–1021 (2009)

Journal of Cellular Biochemistry

Subcellular Localization and Phosphorylation of Antizyme 2

Noriyuki Murai,* Akihiro Shimizu, Yasuko Murakami, and Senya Matsufuji

Department of Molecular Biology, The Jikei University School of Medicine, 3-25-8 Nishi-shinbashi, Minato-ku, Tokyo 105-8461, Japan

ABSTRACT

Antizymes (AZs) are polyamine-induced proteins that negatively regulate cellular polyamine synthesis and uptake. Three antizyme isoforms are conserved among mammals. AZ1 and AZ2 have a broad tissue distribution, while AZ3 is testis specific. Both AZ1 and AZ2 inhibit ornithine decarboxylase (ODC) activity by binding to ODC monomer and target it to the 26S proteasome at least in vivo. Both also inhibit extra-cellular polyamine uptake. Despite their being indistinguishable by these criteria, we show here using enhanced green fluorescent protein (EGFP)-AZ2 fusion protein that in mammalian cells, the subcellular location of AZ2 is mainly in the nucleus, and is different from that of AZ1. The C-terminal part of AZ2 is necessary for the nuclear distribution. Within a few hours, a shift in the distribution of EGFP-AZ2 fusion protein from cytoplasm to the nucleus or from nucleus to cytoplasm is observable in NIH3T3 cells. In addition, we found that in cells a majority of AZ2, but not AZ1, is phosphorylated at Ser-186, likely by protein kinase CK2. There may be a specific function of AZ2 in the nucleus. J. Cell. Biochem. 108: 1012–1021, 2009.

KEY WORDS: ANTIZYME; SUBCELLULAR LOCALIZATION; PHOSPHORYLATION; ORNITHINE DECARBOXYLASE

Antizyme is a polyamine-induced protein that negatively regulates polyamine synthesis and uptake [Heller et al., 1976; Hayashi et al., 1996; Coffino, 2001]. There are three antizyme isoforms conserved among mammals. AZ1 and AZ2 have a broad tissue distribution, while AZ3 is testis specific [Ivanov et al., 2000; Tosaka et al., 2000]. The synthesis of all three antizyme requires a specific ribosomal frameshift that is stimulated by polyamines [Matsufuji et al., 1995]. AZ1 binds to ornithine decarboxylase (ODC), inhibits its activity [Li and Coffino, 1994] and accelerates the degradation of ODC by the 26S proteasome without ubiquitination [Murakami et al., 1992]. AZ2 essentially shares these activities [Zhu et al., 1999], except that AZ2 stimulates ODC degradation only in cells, but not in a rabbit reticulocyte lysate system [Zhu et al., 1999; Chen et al., 2002]. In addition, both AZ1 and AZ2 inhibit cellular polyamine uptake and bind to antizyme inhibitor (AZIn) 1 and 2, proteins that are homologous to ODC but lack its catalytic activity [Zhu et al., 1999; Mangold and Leberer, 2005; Kanerva et al., 2008; López-Contreras et al., 2009].

One of a small number of genes upregulated by seizure-inducing substrate in neuronal cells [Kajiwara et al., 1996] was later identified to be an antizyme gene and termed antizyme 2 [Ivanov et al., 1998]. Although its function appears to be very similar to AZ1, AZ2 is evolutionally more conserved across species than AZ1 does despite its lower expression level [Ivanov and Matsufuji, in press].

These characteristics suggest that AZ2 has unique functions distinct from AZ1. In the present study, we show that the subcellular localization of AZ2 is different from AZ1 and that AZ2, unlike AZ1, is mostly phosphorylated at a specific residue.

MATERIALS AND METHODS

PLASMID CONSTRUCTION AND SITE DIRECTED MUTAGENESIS

To generate AZ1 and AZ2 constructs fused with EGFP at the N-terminus, an *Xho*I/*Eco*RI DNA fragment encoding EGFP was amplified by polymerase chain reaction (PCR) from the pd2EGFP-N1 vector (Clontech). *Eco*RI/*Xba*I DNA fragments encoding in-frame mutant forms of rat AZ1ΔT and mouse AZ2ΔT coding regions were amplified by PCR from pGEM4Z/ΔT205 [Matsufuji et al., 1995] and pTZ19U/AZ-2if [Ivanov et al., 1998], respectively. These fragments were inserted in tandem into the *Xho*I and *Xba*I restriction sites of pd2EGFP-N1 vector (Clontech), resulting in pEGFP-AZ1 and pEGFP-AZ2. To generate plasmids pCMV-HA-AZ1 and pCMV-HA-AZ2, *Eco*RI/*Kpn*I DNA fragments encoding rat AZ1ΔT and mouse

Grant sponsor: Takeda Science Foundation; Grant sponsor: Jikei University Research Funds; Grant sponsor: Jikei University Graduate Research Fund.

*Correspondence to: Dr. Noriyuki Murai, Department of Molecular Biology, The Jikei University School of Medicine, 3-25-8 Nishi-shinbashi, Minato-ku, Tokyo 105-8461, Japan. E-mail: nmurai@jikei.ac.jp

Received 25 May 2009; Accepted 3 August 2009 • DOI 10.1002/jcb.22334 • © 2009 Wiley-Liss, Inc.
Published online 1 September 2009 in Wiley InterScience (www.interscience.wiley.com).

AZ2ΔT were amplified as above and inserted into the *Eco*RI/*Kpn*I sites of the pCMV-HA vector (Clontech). To generate a plasmid pCMV-HA-ODC, *Eco*RI/*Kpn*I DNA fragments encoding mouse ODC coding regions were amplified from pODC20.7 [Gupta and Coffino, 1985] and inserted into the *Eco*RI/*Kpn*I sites of pCMV-HA. Mouse AZIn 1 cDNA was amplified by PCR from mouse kidney cDNA library (Clontech). To generate plasmids p3xFLAG-ODC and p3xFLAG-AZIn, *Eco*RI–*Bgl*II DNA fragments encoding mouse ODC and mouse AZIn 1 were amplified as above and inserted into the *Eco*RI/*Bgl*II sites of the p3xFLAG-CMV-7.1 vector (Sigma). Site-directed mutagenesis was performed using the Quick Change Kit (Stratagene) to generate a series of mutations (S170A, S186A, S170A/S186A, and S186E) at putative phosphorylation sites of AZ2. To generate pGST-AZ2, pGST-AZ2$_{S170A}$ and pGST-AZ2$_{S186A}$, cDNAs of AZ2ΔT and its mutants were subcloned into pGEX4T-1 (Amersham Bioscience) bacterial expression vector. All constructs were verified by sequencing with an ABI PRISM 3700 sequencer and Big Dye® terminator v3.1 cycle-sequencing kit (ABI).

CELL CULTURE

Mouse NIH3T3, African green monkey COS-7, and mouse Neuro2a cells were obtained from ATCC. NIH3T3 cells were maintained in Dulbecco's modified Eagle's medium (DMEM) containing 10% calf serum. COS-7 and Neuro2a cells were cultured in DMEM supplemented with 10% fetal calf serum (FCS) and non-essential amino acid mixture (GIBCO). These three cells were grown at 37°C in a humidified 5% CO_2 atmosphere. Suspension 293-F cells (Invitrogen) were cultured in FreeStyle™ 293 Expression Medium (Invitrogen) in a 37°C incubator under a humidified 8% CO_2 atmosphere with Erlenmeyer flasks rotating at 135 rpm.

TRANSFECTION

Plasmid DNA was purified for transfection using Plasmid Mini Kit (QIAGEN). NIH3T3, COS-7 and Neuro2a cells were seeded in 35-mm polystyrene dishes or on glass bottom dishes (IWAKI) and transiently transfected at 50–70% confluency with 1 μg of plasmid DNA using Lipofectamine and Plus reagent (Invitrogen). 293-F cells were transfected at concentration of 3×10^6 to 1×10^7 cells/ml with 5 μg of plasmid DNA using 293fectin™ (Invitrogen).

ANTIBODIES

Anti-HA polyclonal and monoclonal antibody were purchased from Medical & Biological Laboratories (MBL) and Cell Signaling Technology, respectively. Anti-HA antibody-conjugated agarose were purchased from MBL. Anti-FLAG antibody (M2) and anti-FLAG antibody (M2)-agarose were from Sigma. Anti-S186-phosphorylation specific polyclonal antibody (anti-P-S186) was raised in rabbits against a synthesized AZ2 peptide (the C-terminal 12 amino acid residues of phosphorylated form of mouse AZ2: CYPLDQNLpSDED, where pS denotes a phosphoserine residue). The anti-P-S186 antibody was purified from anti-serum with absorption by a non-phosphorylated AZ2 peptide column and with a protein A agarose column.

FLUORESCENCE MICROSCOPY

EGFP fusion proteins in living cells were visualized using an Olympus IX70 inverted fluorescence microscope equipped with a Polaroid PDMC Ie digital camera 24 h after transfection unless otherwise indicated. Nuclear DNA was stained with 100 ng/ml of Hoechst 33342 (Molecular Probes) for 90 min under the culture conditions. After staining, cells were washed twice with fresh medium and incubated for 1 h before observation. For immunocytochemical detection of HA-tagged proteins, cells were seeded on glass-bottom plates and transfected as above. Twenty-four hours after transfection, cells were fixed in 4% paraformaldehyde at 4°C for 4 h and permeabilized on ice using pre-chilled methanol (−20°C) for 10 min. Aldehyde groups were quenched by incubating the cells with 10 mM glycine (pH 8.5) at room temperature for 5 min. Fixed cells were incubated in blocking solution (3% pre-immune goat serum in phosphate-buffered saline (PBS)) at room temperature for 1 h and then with anti-HA monoclonal antibody diluted 1:500 in blocking solution at room temperature for 1 h or at 4°C overnight. HA-tagged proteins were detected using monoclonal anti-IgG antibodies conjugated with Alexafluoro-545 fluorescence probes (Molecular Probes).

PREDICTION OF PHOSPHORYLATION SITES

Phosphorylation sites of AZ2 were predicted using PredictProtein, a service for sequence analysis, structure and function prediction (http://www.predictprotein.org/).

IMMUNOPRECIPITATION AND IMMUNOBLOT ANALYSES

Cells were washed twice in PBS and suspended in CelLytic™M Cell Lysis Reagent (Sigma) supplemented with a proteinase inhibitor cocktail (Sigma). The cell suspension was sonicated for 1 min and centrifuged at 12,000*g* at 4°C for 20 min. The supernatants containing an equal amount of protein extract were separated by SDS–PAGE and protein bands were electrotransferred to Hybond-P PVDF membrane (GE Healthcare). Immunodetection was carried out with anti-HA and anti-FLAG polyclonal antibodies at dilutions of 1:2,000 and 1:20,000, respectively. Anti-rabbit IgG conjugated horseradish peroxidase (GE Healthcare) was used as the secondary antibody. The proteins were visualized using ECL-Plus Western blotting detection system (GE Healthcare). Bacterial alkaline phosphatase (Takara) was used to confirm the phosphorylation of AZ2.

SEPARATION OF PHOSPHORYLATED AZ2 PROTEIN

Cell extracts prepared from 293F cells expressed 3xFLAG-ODC and HA-AZ2 were immunoprecipitated with anti-FLAG (M2) antibody conjugated agarose. A portion of immunoprecipitate was treated with bacterial alkaline phosphatase for 75 min at 37°C. Separation of SDS–PAGE was prolonged to 140 min.

ODC AND AZIN BINDING ASSAY

Suspension 293-F cells were transfected with 3xFLAG-ODC or 3xFLAG-AZIn, either alone or in combination with HA-AZ2, HA-AZ2$_{S186A}$, or HA-AZ2$_{S186E}$. The cells were harvested by

centrifugation at 1,800 rpm for 5 min, washed twice in PBS and suspended in CelLytic™M Cell Lysis Reagent (Sigma) containing proteinase inhibitor cocktail (Sigma). The cell suspensions were sonicated for 1 min and centrifuged at 15,000 rpm. The supernatants were immunoprecipitated with either anti-FLAG agarose, anti-HA agarose, or anti-HA monoclonal antibody and protein G beads (Invitrogen). One-tenth volume of the lysate was used to analyze input protein level by Western blotting using anti-HA or anti-FLAG antibody. The proteins were detected with immunoblot analysis as described above.

IN VIVO PHOSPHORYLATION ASSAY

NIH3T3 cells transiently expressing HA-tagged AZ1 or AZ2 were labeled with [^{32}P]orthophosphate (0.5 mCi/ml) in phosphate-free medium supplemented with 10% FCS which had been dialyzed against saline. After incubation for 3 h, the cells were washed twice with PBS and lysed with RIPA buffer (20 mM Tris–HCl pH7.4, 0.15 M NaCl, 0.5 M EDTA, 1% NP-40, 1% deoxycholate, 0.1% SDS, 50 mM NaF, 10 μg/ml aprotinin, and 10 μg/ml leupeptin) supplemented with protease inhibitor cocktail. The cell lysates were immunoprecipitated with anti-HA antibody-conjugated agarose. The agarose was collected by centrifugation at 5,000 rpm for 5 min and washed 5 times with RIPA buffer. Immunoprecipitates were eluted by NuPAGE® LSD sample buffer (Invitrogen) and separated by SDS–PAGE in duplicate. Radiolabeled proteins were visualized using a fluorescence imaging analyzer FLA2000. Total HA-AZ2 and its mutant proteins were detected by immunoblotting using anti-HA polyclonal antibody.

IN VITRO PHOSPHORYLATION ASSAY

Glutathione-*S*-transferase (GST) fusion protein was expressed in *E. coli* BL21 carrying pGST-AZ2, pGST-AZ2$_{S170A}$ or pGST-AZ2$_{S186A}$, and purified with glutathione-Sepharose 4B beads (GE Healthcare). In vitro phosphorylation reaction was performed in a mixture containing 20 mM Tris–HCl, pH 8.0, 200 mM NaCl, 2 mM ATP, 1 mM dithiothreitol (DTT), 1.85 MBq of [γ-^{32}P]ATP and 250 U of purified protein kinase CK2 (CK2, formerly casein kinase II) (NEB) at 37°C for 1 h. Radiolabeled proteins were separated on a 4–12% gradient SDS–PAGE gel and visualized using FLA2000.

IN VIVO ODC DEGRADATION ASSAY

Suspension 293-F cells were transfected with pCMV-HA-ODC either alone or in combination with pCMV-HA-AZ2, pCMV-HA-AZ2$_{S186A}$ or pCMV-HA-AZ2$_{S186E}$. Twenty-four hours after transfection, cycloheximide was added to the medium and at indicated time points cells were harvested by centrifugation at 1,800 rpm for 3 min. The cells were lysed and immunoprecipitated with ProFound™ Mammalian HA Tag IP/Co-IP Kit (Pierce). HA-tagged ODC was detected by immunoblot analysis using anti-HA polyclonal antibody.

ASSAY OF SPERMIDINE UPTAKE

Suspension 293-F cells were transfected with pCMV-HA-AZ1, pCMV-HA-AZ2, pCMV-HA-AZ2$_{S186A}$, pCMV-HA-AZ2$_{S186E}$ or pd2EGFP-N1 (negative control). The cells were incubated in 5 ml of FreeStyle™ 293 Expression Medium in Erlenmeyer flasks rotating at 135 rpm for 24 h, and then transferred to 60 mm dishes and incubated in the same medium containing 5 μM [^{14}C] spermidine (125 nCi) at 37°C for 30 min. Polyamine uptake was terminated by washing the cells with ice-cold PBS five times. Cells were lysed with 0.1% SDS, at 0.1 ml/dish, and radioactivity determined in a scintillation counter. Uptake activity was designated as CPM/dish.

RESULTS

SUBCELLULAR DISTRIBUTION OF AZ2

We first compared the subcellular localization of AZ2 with that of AZ1. NIH3T3 cells were transiently transfected with the EGFP-AZ1 or EGFP-AZ2 expression vector, and analyzed by fluorescence microscopy. As we previously reported, EGFP-AZ1 was predominantly localized in the cytoplasm (Fig. 1A) [Murai et al., 2003]. In contrast, the distribution of EGFP-AZ2 split into two patterns; a nuclear dominant distribution (N) and a diffuse distribution in both cytoplasm and nucleus (NC) (Fig. 1B). To confirm the result, AZ2 was expressed with a small epitope, HA (HA-AZ2), in NIH3T3 cells and detected immunohistochemically. HA-AZ2 was also distributed in two patterns (Fig. 1B). The distribution of AZ2 in COS-7 and Neuro-2a cells was also examined using ECFP-Tagged AZ2 (Fig. 1C). The distribution patterns were essentially the same as that in NIH3T3 cells, but the proportion of the nuclear dominant distribution was higher in both COS-7 and Neuro-2a cells than in NIH3T3 cells. In a closer observation, the nuclear distribution of EGFP-AZ2 in NIH-3T3 cells was not uniform, being limited to the non-condensed chromatin area stained only weakly by Hoechst 33342. Further, in tracking observations, the fluorescent intensity of EGFP-AZ2 gradually accumulated into the nucleus or diffused away from the nucleus within a few hours in some cells, indicating that EGFP-AZ2 shuttles between the nucleus and the cytoplasm (Fig. 1D).

To determine which amino acid residues are essential for nuclear localization, we prepared constructs encoding three separate segments of the AZ2 (amino acid residues 1–32, 33–97, and 98–189, respectively), fused with the C-terminus of EGFP. The constructs were expressed in NIH3T3 cells. A quantitative analysis of the distribution of EGFP-AZ2 showed that about 30% of cells had the N pattern and the rest had the NC pattern (Fig. 2, left panel). EGFP-AZ2$_{98-189}$ was distributed predominantly in the nucleus in 60% of cells; a proportion that is even higher than that of full-length EGFP-AZ2. In contrast, EGFP-AZ2$_{1-32}$ and EGFP-AZ2$_{33-97}$ were diffusely localized in both the cytoplasm and nucleus of most of the cells. These results indicate that amino acid residues 98–189 of AZ2 contain a signal necessary for the nuclear distribution of AZ2. We further tried to determine a minimal region which is sufficient for nuclear localization, but additional deletions made the protein products aggregate in cells.

PHOSPHORYLATION OF AZ2

Since the nuclear accumulation of AZ2 is possibly regulated, and such regulation is often mediated by protein phosphorylation, we

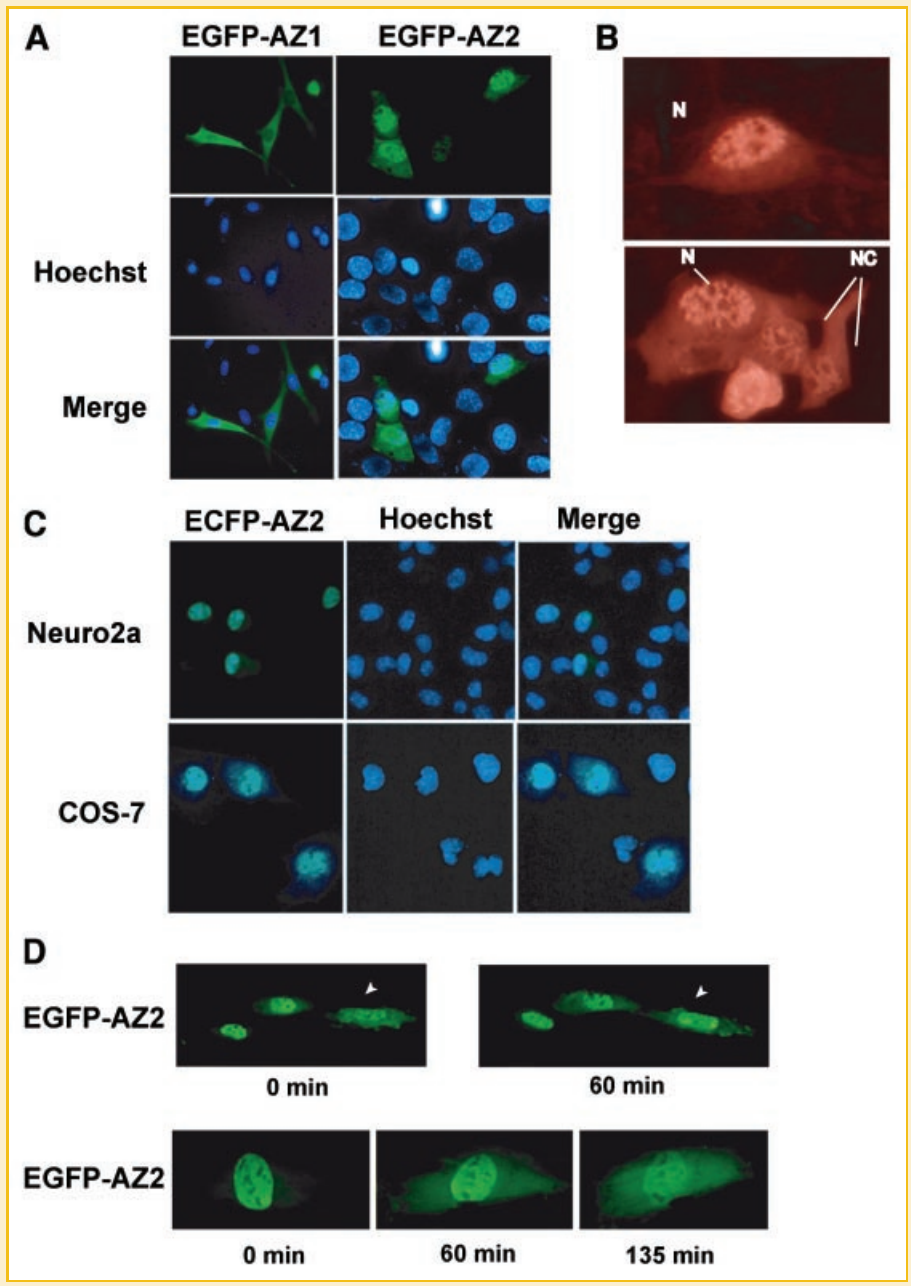

Fig. 1. Subcellular localization of AZ2 in mammalian cells. A: Expression of EGFP-AZ1 or EGFP-AZ2 in transiently transfected NIH3T3 cells with the nuclei stained with Hoechst 33342 and visualized with fluorescence microscopy. B: Location of HA-AZ2 synthesized in transiently transfected NIH3T3 cells analyzed by indirect immunofluorescence using antibodies against HA epitope tags and fluorescein-conjugated secondary antibody. "N" denotes predominantly nuclear localization and "NC" denotes even distribution in the cytoplasm and nucleus. C: ECFP-AZ2 synthesized in transiently transfected COS-7 and Neuro2a cells with the fluorescent color of ECFP replaced by emerald green and using software to distinguish fluorescence of Hoechst 33324 from that of ECFP. D: Temporary shift of EGFP-AZ2 localization. EGFP-AZ2 synthesized in transiently transfected NIH3T3 cells with live-cell images observed by fluorescence microscopy after 24 h and indicated intervals thereafter. In the upper panels, the cell showing a shift of EGFP-AZ2 is marked with an arrowhead.

examined whether AZ2 is phosphorylated or not. NIH3T3 cells transiently expressing HA-tagged AZ1 (HA-AZ1) or HA-AZ2, were incubated in the presence of [^{32}P]orthophosphate for 3 h and labeled bands were analyzed by SDS–PAGE followed by autoradiography. A band of the corresponding size was detected only in HA-AZ2 expressing cells (Fig. 3A). This indicates that AZ2, but not AZ1, is phosphorylated in NIH3T3 cells. A computer analysis revealed that the mouse AZ2 sequence contains several potential phosphorylation sites, and among them, serine-170 and serine-186 of AZ2 were particularly likely candidates for CK2 phosphorylation sites [Meggio and Pinna, 2003]. To determine phosphorylation sites, each of the two residues separately or both were replaced by alanine, fused with

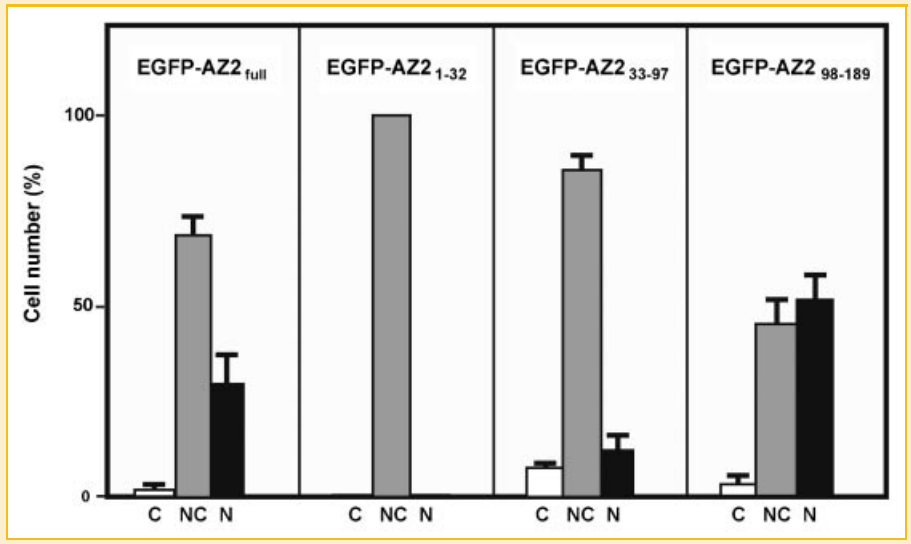

Fig. 2. Quantitation of subcellular distribution of EGFP–AZ2 and its deletion mutants. The indicated AZ2 proteins fused with EGFP were synthesized in transfected NIH3T3 cells and analyzed by fluorescence microscopy. Cellular localization of each fusion protein was scored as: C, predominantly cytoplasm; NC, evenly distributed in the cytoplasm and nucleus; N, predominantly nuclear. For each construct, at least 200 cells were scored from random fields.

an HA-tag (HA-AZ2$_{S170A}$, HA-AZ2$_{S186A}$, or HA-AZ2$_{S170A/S186A}$), and analyzed by autoradiography and immunoblotting. As shown in Figure 4B, HA-AZ2$_{S186A}$ and HA-AZ2$_{S170A/S186A}$ mutants were not labeled, but HA-AZ2$_{S170A}$ was, indicating that serine 186 is the phosphorylated site. Immunoblot analysis using monoclonal anti-HA antibody demonstrated that wild type and mutant HA-AZ2 proteins were all expressed to the same level (Fig. 3B). The phosphorylation of AZ2 with CK2 was further confirmed in vitro. GST-AZ2 and its mutant GST-AZ2$_{S170A}$, synthesized in bacteria, were purified and phosphorylated in the presence of [γ-^{32}P]ATP and purified CK2, but GST-AZ2$_{S186A}$ or GST-AZ2$_{S170A/S186A}$ were not (Fig. 3C). Alignment of mouse AZ2 C-terminal amino acid sequences with those of other species indicated that mouse AZ2 Serine-186 was conserved among vertebrates (Fig. 4).

Next we prepared a serine-186 phosphorylation-specific rabbit polyclonal antibody (anti-P-S186) to detect phosphorylated AZ2 in the cells. HA-AZ2 was expressed in 293F cells together with 3xFLAG-ODC. HA-AZ2 interacting with 3xFLAG-ODC was immunoprecipitated with anti-FLAG agarose, and detected by either anti-HA antibody or anti-P-S186 (Fig. 5). We found that SDS–PAGE with an extended electrophoresis time allows distinction between phosphorylated and non-phosphorylated forms of HA-AZ2: the double bands evident in Figure 5 reflecting separated proteins. Treatment with bacterial alkaline phosphatase resulted in a shift of the product reflected in the upper band to the position of the lower band. Anti-P-S186 detected only the product reflected in the upper band in the phosphatase-untreated sample and very faintly in the phosphatase-treated sample (Fig. 5). Similar results were obtained from the same experiments using calf intestine alkaline phosphatase (data not shown). These results indicate that both phosphorylated and non-phosphorylated forms of AZ2 exist in 293F cells but a majority of AZ2 was phosphorylated. It is also clear that both forms of HA-AZ2 are able to bind to ODC since in the experiment, HA-AZ2 was first co-precipitated with 3xFLAG-ODC.

EFFECT OF AZ2 PHOSPHORYLATION ON SUBCELLULAR LOCALIZATION, ODC BINDING, ODC DEGRADATION, AND AZIN 1 BINDING ACTIVITY

We tested whether the phosphorylation of serine-186 affects the cellular distribution and molecular function of AZ2, since the distribution of some cellular proteins is altered by their phosphorylation [Reich and Liu, 2006]. The phosphorylation-defective AZ2$_{S186A}$ and the phosphorylation-mimicked AZ2$_{S186E}$ mutants were fused with EGFP and expressed in NIH3T3 cells. Observation under a fluorescence microscope revealed, however, that the localization of these mutants was identical to that of wild-type EGFP-AZ2 (data not shown).

Next, we tested binding of AZ2 and its mutants to ODC and AZIn 1. Pull-down assay using anti-FLAG antibody revealed that both AZ2 mutants binds to 3xFLAG-ODC and 3xFLAG-AZIn 1 (Fig. 6A,B). HA-AZ2$_{\mathbf{S186E}}$ was co-precipitated with 3xFLAG-ODC and 3xFLAG-AZIn 1 to the same extent as wild-type HA-AZ2, but amount of co-precipitated HA-AZ2$_{\mathbf{S186A}}$ with 3xFLAG-ODC and 3xFLAG-AZIn 1 was slightly, but reproducibly, less than the products of the other two constructs.

As shown in the second bottom panel of Figure 6A, the level of ODC was markedly decreased in the presence of AZ2 or AZ2 mutants, suggesting that these AZ2 proteins stimulated the degradation of ODC. This was confirmed by a degradation assay, where cycloheximide was added to the culture 24 h after transfection and the level of ODC protein was measured by immunoblot analysis. Both AZ2$_{S186A}$ and AZ2$_{S186E}$ accelerated degradation of ODC with the same efficiency as wild-type AZ2 (Fig. 7A,B).

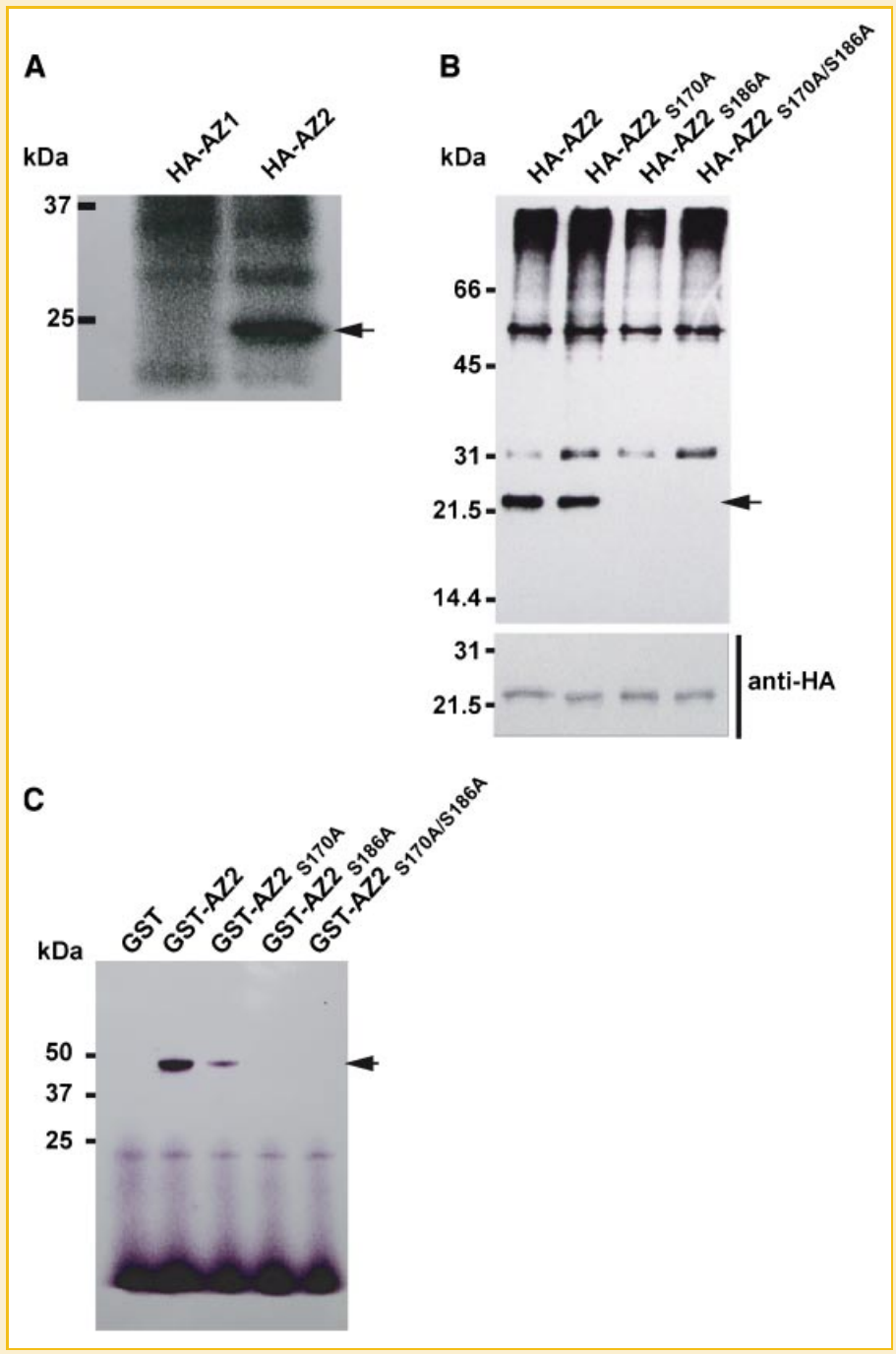

Fig. 3. Phosphorylation of AZ2. A: NIH3T3 cells transiently expressing HA-tagged AZ1 or AZ2 (HA-AZ1 or HA-AZ2) were labeled by [^{32}P]orthophosphate and analyzed by autoradiography. B: NIH3T3 cells were transiently transfected with vectors harboring HA-AZ2 (W), HA-AZ2$_{S170A}$, HA-AZ2$_{S186A}$, or HA-AZ2$_{S170A/S186A}$. Cells were labeled with [^{32}P]orthophosphate and HA-AZ2 proteins were immunoprecipitated with anti HA antibody conjugated with agarose and analyzed by autoradiography. The position of the phosphorylated HA-AZ2 product is indicated by an arrow. The lower panel shows protein expression levels analyzed by immunoblotting using anti-HA antibody. C: In vitro phosphorylation assay of AZ2 and AZ2 mutants. GST and GST-tagged AZ2 proteins (GST-AZ2, GST-AZ2$_{S170A}$, GST-AZ2$_{S186A}$, GST-AZ2$_{S170A/S186A}$) were expressed in *E. coli*, affinity purified and incubated with CK2 and [γ-^{32}P]ATP. Phosphorylation was detected with autoradiography. The position of the phosphorylated HA-AZ2 product is indicated by an arrow.

EFFECT OF AZ2 PHOSPHORYLATION ON INHIBITION OF POLYAMINE UPTAKE

To examine whether AZ2 phosphorylation affects its regulation of polyamine uptake, we performed a spermidine uptake assay in 293-F cells transiently expressing HA-AZ1, HA-AZ2, HA-AZ2$_{S186A}$, HA-AZ2$_{S186E}$ or EGFP (negative control). The expression levels of EGFP and AZ proteins were confirmed to be almost the same (data not shown). As shown in Figure 8, spermidine uptake was inhibited by

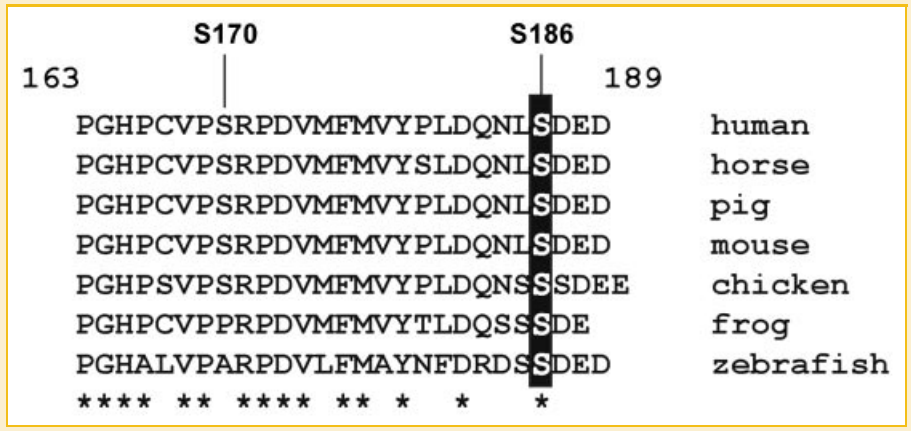

Fig. 4. Alignment of the C-terminal region of AZ2 from various species. The GenBank accession numbers of the aligned C-terminal sequences shown are: human, NM_002537; horse, NM_001130486; pig, EU545196; mouse, NM_010952; chicken, NM_001142862; frog, NM_001095699; and zebrafish, NM_194432. Conserved amino acids among species are denoted by asterisks below the sequences. The serine residue corresponding to sereine-186 in mouse AZ2, is highlighted with a black background.

approximately 50% in cells expressing wild type AZ1, AZ2 and the phosphorylation mutants of AZ2 (Fig. 8). Thus phosphorylation of AZ2 does not alter its inhibitory activity on spermidine uptake.

DISCUSSION

In this study we found two characteristic features of AZ2 which are different from AZ1: (1) AZ2 is mainly distributed in the nucleus in several mammalian cells. (2) In mouse cells, AZ2 is phosphorylated at Ser-186.

In contrast we earlier demonstrated that in mammalian cells AZ1 is mainly distributed in the cytoplasm (Fig. 1) [Murai et al., 2003]. AZ2 tagged with EGFP or HA exhibited two distribution patterns: a nuclear dominant and a diffuse pattern (Fig. 1). The proportion of the patterns was somehow different depending on the cell types. With NIH3T3 cells, approximately 30% of the cells showed the nuclear dominant pattern, but in COS-7 and Neuro2a cells the proportion of the nuclear dominant pattern was more than 70% (Fig. 1C, data not shown). The C-terminal region containing amino acids 98–189 was necessary for nuclear translocation of AZ2, even though this region contains no typical nuclear localization signal (NLS) motif [Dingwall and Laskey, 1991]. Nuclear translocation of AZ2 may be caused by interaction with another molecule that has a nuclear localization signal. Further studies are needed to elucidate the nuclear translocation mechanism of AZ2. We also observed that within hours the distribution of EGFP-AZ2 can shift from the nucleus to cytoplasm or vice versa (Fig. 1D).

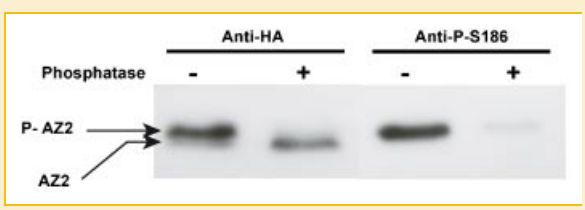

Fig. 5. Separation of phosphorylated and unphosphorylated AZ2 proteins 3xFLAG-ODC and HA-AZ2 were synthesized in cotransfected 293F cells. Cell extracts were immunoprecipitated with anti-FLAG (M2) antibody conjugated agarose. A portion of immunoprecipitate was treated with bacterial alkaline phosphatase. After blotting, HA-AZ2 and its phosphorylated derivative were detected with anti-HA and anti-P-S186 antibodies, respectively. P-AZ2 indicates phosphorylated AZ2.

These localization experiments were performed by forced expression of tagged proteins, and their localization might not be the same as that of the endogenous protein. We attempted to determine the localization of endogenous AZ2, but have not been successful with immunocytochemistry or Western blotting because of insufficient specificity of the currently available antibodies and the extremely low cellular level of AZ2. A reliable method to detect and discriminate endogenous AZ2 should be developed. Nevertheless, the result with AZ2 fused with a small tag, HA, strongly suggests that a substantial proportion of AZ2 is localized in the nucleus. Specific role(s) of AZ2 in the nucleus are likely.

One such function can be acceleration of ODC degradation in the nucleus. ODC is known to be localized both in the nucleus and cytoplasm [Schipper and Verhofstad, 2002; Schipper et al., 2004]. In addition, it was reported that the proteasome inhibitor MG132 led to an accumulation of ODC in the nucleus [Gritli-Linde et al. 2001]. Since proteasomes also occur in the nucleus [Voss and Grune, 2007], AZ2 may bind to ODC and target it to nuclear proteasomes. It has been reported that AZ2 cannot stimulate ODC degradation in vitro, but only in living cells [Zhu et al., 1999; Snapir et al., 2009]. This may be due to the difference in localization of the two antizymes demonstrated in this work. AZ1 and AZ2 may play distinct roles in stimulating ODC degradation in discrete compartments of the cell.

Nuclear AZ2 may exert an additional role other than regulating ODC. Recent reports indicated that both AZ1 and AZIn 1 are localized in the centrosome and affect centrosome amplification [Mangold et al., 2008]. It is reported that AZ1 also mediates

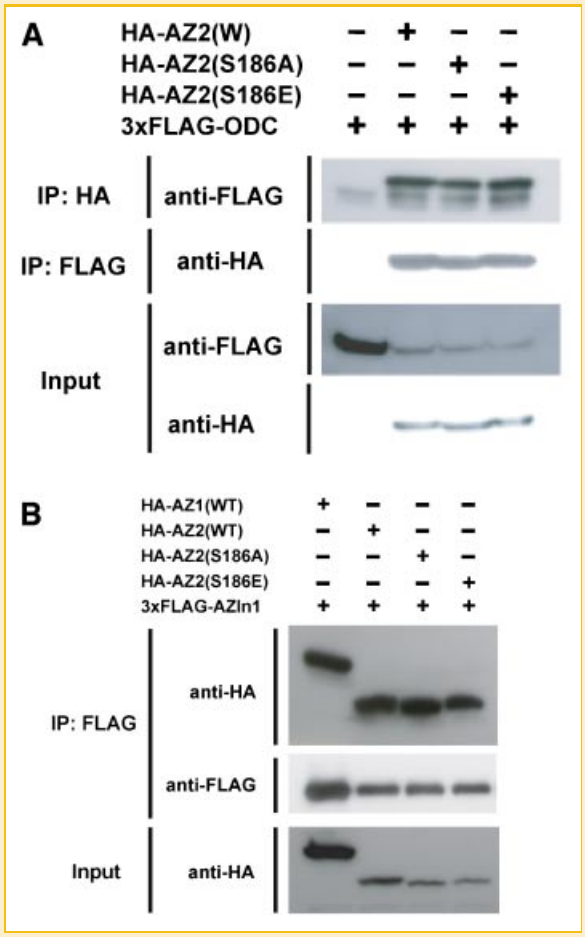

Fig. 6. Binding of the phosphorylation site mutants of AZ2 to ODC and AZIn 1. A: Pull-down assay for binding to ODC. 293F cells were cotransfected with 3xFLAG-ODC and one of HA-AZ2, HA-AZ2$_{S186A}$, or HA-AZ2$_{S186E}$ encoding plasmids. The cell lysates were immunoprecipitated with either anti-HA antibody or anti-FLAG agarose, and tagged proteins were detected with anti-FLAG antibody or anti-HA antibody in the Western blot shown. B: Pull-down assay for binding to AZIn 1. 293F cells were cotransfected with 3xFLAG-AZIn 1 and one of HA-AZ2, HA-AZ2$_{S186A}$, or HA-AZ2$_{S186E}$ encoding plasmids and analyzed as in A except that immunoprecipitation was performed using only anti-FLAG agarose.

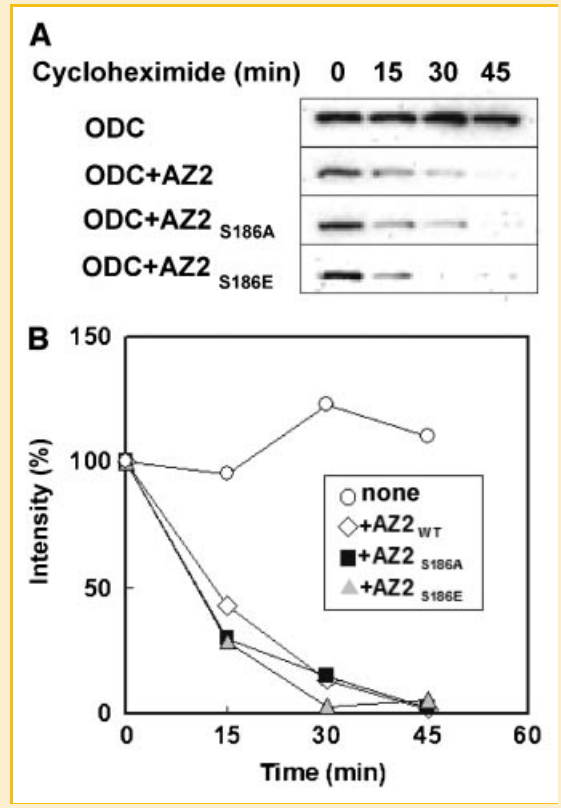

Fig. 7. Stimulation of ODC degradation by AZ2 phosphorylation site mutants (A) 293F cells were transfected with pCMV-HA-ODC alone or together with one of pCMV-HA-AZ2, pCMV-HA-AZ2$_{S186A}$, or pCMV-HA-AZ2$_{S186E}$ encoding plasmids. Cycloheximide was added to the medium 24 h after transfection and cells were collected at the indicated times. ODC was detected on immunoblot analysis using anti HA antibody. B: The intensity of ODC bands was quantified using an immuno image analyzer and presented as % of the initial intensity.

AURKAIP1-dependent degradation of Aurora-A oncogene in cells and in reticulocyte lysates [Lim and Gopalan, 2007]. Other nuclear proteins have also been reported to interact with AZ1 [Wang, 2003; Newman et al., 2004]. These findings raise the possibility that AZ2 has an additional binding partner in the nucleus.

The nuclear distribution of EGFP-AZ2 in NIH-3T3 cells was not uniform and limited at the non-condensed area of chromatin (Fig. 1A). In such areas, histones are highly modified by enzymes such as lysine acetyltransferase and lysine methyltransferase, resulting in activation of transcription. The histone modifications are controlled by the balanced activities of lysine acetyltransferase/histone deacetylases, and lysine methyltransferase/demethylases, respectively [Thorne et al., 2009]. These enzymes use acetyl CoA and *S*-adenosylmethionine as acetyl- and methyl-donors, respectively, and both of these metabolites are also involved in polyamine biosynthesis and catabolism [Jell et al., 2007]. Indeed, polyamine analogs can inhibit the activity of lysine demethylases [Thorne et al., 2009]. It is therefore plausible that AZ2 may be involved in regulating histone modification enzymes, transcription factors or kinases either through regulation of the local polyamine content or by a more direct manner. A search for novel AZ2 interacting molecules is underway in our laboratory using a two-hybrid system.

We discovered that the majority of AZ2 in cells is phosphorylated (Figs. 3A and 5). An amino acid substitution analysis revealed that serine-186 is the phosphorylation site (Fig. 3B,C), and the sequence surrounding this residue matches the consensus of CK2 substrate sites. Indeed recombinant AZ2 was phosphorylated by CK2 in vitro. Comparison of C-terminal sequences of mouse AZ2 and AZ1 with that of other species indicated that serine-186 was conserved in AZ2 among vertebrates (Fig. 5), but mouse and zebrafish AZ1 do not contain the corresponding residue, suggesting that the phosphorylation at this residue is a unique feature of AZ2.

We examined the effect of Ser-186 phosphorylation. However, neither the subcellular localization of AZ2 (data not shown), activities of AZ2 such as ODC binding, acceleration of ODC

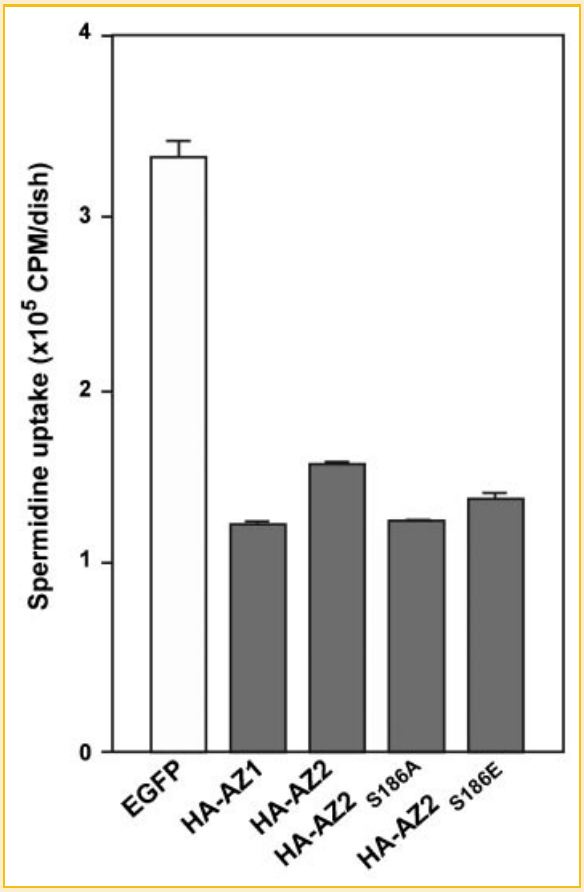

Fig. 8. Inhibition of polyamine uptake of phosphorylation site mutants of AZ2 HA tagged AZ1, AZ2, AZ2$_{S186A}$, AZ2$_{S186E}$, or EGFP (control) were synthesized in transfected 293F cells. The cells were later incubated in a medium containing 5 μM [^{14}C]spermidine (125 nCi) at 37°C for 30 min, and polyamine uptake terminated by washing the cells with cold PBS. Lysed cells were used for radioactive content. Transport activity was designated as CPM/dish.

degradation, AZIn 1 binding and inhibition of polyamine uptake, (Figs. 6–8), nor stability of AZ2 (data not shown) were affected by mutating Ser-186 to alanine or aspartate. Ser-186 phosphorylation is thus considered to be silent for these characteristics of AZ2. Similar physiologically silent phosphorylation is also known for mammalian ODC [Rosenberg-Hasson et al., 1991]. However, it is still possible that the phosphorylation is important for the interaction of AZ2 with an unknown partner.

ACKNOWLEDGMENTS

We thank Dr. J.F. Atkins for his comments on the manuscript and Dr. I.P. Ivanov for the plasmid pTZ19U/AZ-2if.

REFERENCES

Chen H, MacDonald A, Coffino P. 2002. Structural elements of antizymes 1 and 2 are required for proteasomal degradation of ornithine decarboxylase. J Biol Chem 277:45957–45961.

Coffino P. 2001. Regulation of cellular polyamines by antizyme. Nature Rev Mol Cell Biol 2:188–194.

Dingwall C, Laskey RA. 1991. Nuclear targeting sequences—A consensus? Trends Biochem Sci 16:478–481.

Gritli-Linde A, Nilsson J, Bohlooly YM, Heby O, Linde A. 2001. Nuclear translocation of antizyme and expression of ornithine decarboxylase and antizyme are developmentally regulated. Dev Dyn 220:259–275.

Gupta M, Coffino P. 1985. Mouse ornithine decarboxylase. Complete amino acid sequence deduced from cDNA. J Biol Chem 260:2941–2944.

Hayashi S, Murakami Y, Matsufuji S. 1996. Ornithine decarboxylase antizyme: A novel type of regulatory protein. Trends Biochem Sci 21: 27–30.

Heller JS, Fong WF, Canellakis ES. 1976. Induction of a protein inhibitor to ornithine decarboxylase by the end products of its reaction. Proc Natl Acad Sci USA 73:1858–1862.

Ivanov IP, Matsufuji S. in press. Autoregulatory frameshifting in antizyme gene expression governs polyamine levels from yeast to mammals. In: Atkins JF, Gesteland RF, editors. Recoding: Expansion of decoding rules enriches gene expression. New York: Springer.

Ivanov IP, Gesteland RF, Atkins JF. 1998. A second mammalian antizyme: Conservation of programmed ribosomal frameshifting. Genomics 52:119–129.

Ivanov IP, Rohrwasser A, Terreros D, Gesteland RF, Atkins JF. 2000. Discovery of a spermatogenesis stage-specific ornithine decarboxylase antizyme: Antizyme 3. Proc Natl Acad Sci USA 97:4808–4813.

Jell J, Merali S, Hensen ML, Mazurchuk R, Spernyak JA, Diegelman P, Kisiel ND, Barrero C, Deeb KK, Alhonen L, Patel MS, Porter CW. 2007. Genetically altered expression of spermidine/spermine N^1-acetyltransferase affects fat metabolism in mice via acetyl-CoA. J Biol Chem 282:8404–8413.

Kajiwara K, Nagawawa H, Shimizu-Nishikawa K, Ookura T, Kimura M, Sugaya E. 1996. Molecular characterization of seizure-related genes isolated by differential screening. Biochem Biophys Res Commun 21:9795–9799.

Kanerva K, Mäkitie LT, Pelander A, Heiskala M, Andersson LC. 2008. Human ornithine decarboxylase paralogue (ODCp) is an antizyme inhibitor but not an arginine decarboxylase. Biochem J 409:187–192.

Li X, Coffino P. 1994. Distinct domains of antizyme required for binding and proteolysis of ornithine decarboxylase. Mol Cell Biol 14:87–92.

Lim SK, Gopalan G. 2007. Antizyme 1 mediates AURKAIP1-dependent degradation of Aurora-A. Oncogene 26:6593–6603.

López-Contreras AJ, Sánchez-Laorden BL, Ramos-Molina B, de la Morena ME, Cremades A, Peñafiel R. 2009. Subcellular localization of antizyme inhibitor 2 in mammalian cells: Influence of intrinsic sequences and interaction with antizymes. J Cell Biochem 107:732–740.

Mangold U, Leberer E. 2005. Regulation of all members of the antizyme family by antizyme inhibitor. Biochem J 385:21–28.

Mangold U, Hayakawa H, Coughlin M, Münger K, Zetter BR. 2008. Antizyme, a mediator of ubiquitin-independent proteasomal degradation and its inhibitor localize to centrosomes and modulate centriole amplification. Oncogene 27:604–613.

Matsufuji S, Matsufuji T, Miyazaki Y, Murakami Y, Atkins JF, Gesteland RF, Hayashi S. 1995. Autoregulatory frameshifting in decoding mammalian ornithine decarboxylase antizyme. Cell 80:1360–1370.

Meggio F, Pinna LA. 2003. One-thousand-and-one substrates of protein kinase CK2? FASEB J 17:349–368.

Murai N, Murakami Y, Matsufuji S. 2003. Identification of nuclear export signals in antizyme-1. J Biol Chem 278:44791–44798.

Murakami Y, Matsufuji S, Kameji T, Hayashi S, Igarashi K, Tamura T, Tanaka K, Ichihara A. 1992. Ornithine decarboxylase is degraded by the 26S proteasome without ubiquitination. Nature 360:597–599.

Newman RM, Mobascher A, Mangold U, Koike C, Diah S, Schmidt M, Finley D, Zetter BR. 2004. Antizyme targets cyclin D1 for degradation. A novel mechanism for cell growth repression. J Biol Chem 279:41504–41511.

Reich NC, Liu L. 2006. Tracking STAT nuclear traffic. Nat Rev Immunol 6:602–612.

Rosenberg-Hasson Y, Strumpf D, Kahana C. 1991. Mouse ornithine decarboxylase is phosphorylated by casein kinase-II at a predominant single location (serine 303). Eur J Biochem 197:419–424.

Schipper RG, Verhofstad AA. 2002. Distribution patterns of ornithine decarboxylase in cells and tissues: Facts, problems, and postulates. J Histochem Cytochem 50:1143–1160.

Schipper RG, Cuijpers VM, De Groot LH, Verhofstad AA. 2004. Intracellular localization of ornithine decarboxylase and its regulatory protein, antizyme-1. J Histochem Cytochem 52:1259–1266.

Snapir Z, Keren-Paz A, Bercovich Z, Kahana C. 2009. Antizyme 3 inhibits polyamine uptake and ornithine decarboxylase (ODC) activity, but does not stimulate ODC degradation. Biochem J 419:99–103.

Thorne JL, Campbell MJ, Turner BM. 2009. Transcription factors, chromatin and cancer. Int J Biochem Cell Biol 41:164–175.

Tosaka M, Okajima F, Hashiba Y, Saito N, Nagano T, Watanabe T, Kimura T, Sasaki T. 2000. Identification and characterization of testis specific ornithine decarboxylase antizyme (OAZ-t) gene: Expression in haploid germ cells and polyamine-induced frameshifting. Genes Cells 5:265–276.

Voss P, Grune T. 2007. The nuclear proteasome and the degradation of oxidatively damaged proteins. Amino Acids 32:527–534.

Wang T. 2003. The 26S proteasome system in the signaling pathways of TGF-beta superfamily. Front Biosci 8:1109–1127.

Zhu C, Lang DW, Coffino P. 1999. Antizyme 2 is a negative regulator of ornithine decarboxylase and polyamine transport. J Biol Chem 274:26425–26430.